The Class II/III Transition in Triarylamine Redox Systems

Christoph Lambert* and Gilbert Nöll

Contribution from the Institut für Organische Chemie, Universität Regensburg, Universitätsstraße 31, D-93040 Regensburg, Germany

Received April 20, 1999

Abstract: The mixed-valence character of a set of six bistriarylamine derivatives with varying π-electron spacers has been investigated. The distances of triarylamine redox centers vary from 0.5 nm (N,N,N',N'-tetra-4-methoxyphenyl-*p*-phenylenediamine, $\mathbf{6}^+$) to 2 nm (1,4-bis{4-[N,N-di(4-methoxyphenyl)amino]phenylethynyl}-benzene, $\mathbf{1}^+$). All radical cation species show rather strong intervalence charge-transfer (IV–CT) bands in the NIR as measured by UV/vis/NIR spectroelectrochemistry. Hush analysis was used to derive the electronic coupling V, which is very high and ranges from 500 to 3240 cm^{-1}. A detailed band shape analysis revealed a cutoff at $2V$ at the low-energy side of the IV–CT bands when the coupling $2V$ approaches the band maximum λ. This results in very narrow IV–CT bands much smaller than the high-temperature limit, although even the phenylenediamine derivative $\mathbf{6}^+$ belongs to the Robin/Day class II (localized redox centers) just at the border to class III (delocalized redox centers). Hush theory anticipates this cutoff because the smallest energy transition possible is at $2V$. The ultrafast thermal electron-transfer rate constants were estimated from V and range from about 10^9 s^{-1} to 10^{12} s^{-1}. The electrochemical properties have also been investigated: a linear correlation of redox potential splitting vs electronic coupling was found.

Introduction

Electron-transfer (ET) reactions are one of the most fundamental processes in chemistry[1] and biology.[2] Thus, numerous investigations were devoted to the study of ET processes in real biological systems,[3] in biomimetic model compounds,[4] and in structurally simple and completely artificial low molecular weight systems.[5] The aims reach from the desire to understand ET processes in nature to the design of molecular wires for electronic communication.[6] Since the seminal work of Creutz and Taube on mixed-valence compounds, these, compared to natural ET systems, simple inorganic derivatives were used as test cases in order to study basic aspects of ET theories,[7] that is, to check the applicability of Marcus ET theory and its extension, the Hush theory for interpreting intervalence charge-transfer (IV–CT) absorption spectra.[8] In 1967, Robin and Day[9] classified mixed-valence compounds with two (or more) redox centers into three categories: (a) the redox centers are com-

pletely localized and behave as separate entities (class I), (b) intermediate coupling between the mixed valence centers exists (class II), and finally, (c) class III derivatives where coupling is so strong that the system is completely delocalized and intermediate redox states have to be attributed to the redox centers. The transition between class II and class III systems has recently attracted considerable attention. Meyer at al. investigated pyrazine-[10] and dinitrogen[11]-bridged binuclear osmium complexes, which are at that transition. Ito and Kubiak et al.[12] showed by IR spectroscopy that pyrazine-bridged ruthenium clusters display exceptionally fast ET and are just at the borderline between class II and III. Unfortunately, detailed band shape analyses of the IV–CT absorption bands were hampered in all cases, owing to severe band overlap with other electronic transitions. In the present paper we address the question about what actually happens to the IV–CT absorption band associated with the electron transfer if a system gradually transforms from a true valence-trapped class II situation to a delocalized class III system. The answer might help to elucidate numerous cases where the true electronic nature of the mixed valence compound is not known. For this purpose, we studied a series of bridged triarylamine redox systems (see Chart 1).

According to Marcus,[13,14] the potential energy surface of a degenerate mixed valence system can be constructed from parabolic functions which represent the diabatic (noninteracting) states (Figure 1a). Electronic coupling of these diabatic states leads to an avoided crossing in the intersection region of the

(1) Barbara, P. F.; Meyer, T. J.; Ratner, M. A. *J. Phys. Chem.* **1996**, *100*, 13148.

(2) *Chem. Rev.* **1992**, *92*, 369. This issue is devoted to ET processes in biologically relevant systems.

(3) Moser, C. C.; Keske, J. M.; Warncke, K.; Farid, R. S.; Dutton, P. L. *Nature* **1992**, *355*, 796.

(4) (a) Willner, I.; Willner, B. *Top. Curr. Chem.* **1991**, *159*, 153. (b) Wasielewski, M. R. *Chem. Rev.* **1992**, *92*, 435.

(5) (a) Closs, G. L.; Miller, J. R. *Science* **1988**, *240*, 440. (b) Paddon-Row, M. N. *Acc. Chem. Res.* **1994**, *27*, 18.

(6) (a) Tolbert, L. M.; Zhao, X.; Ding, Y.; Bottomley, L. A. *J. Am. Chem. Soc.* **1995**, *117*, 12891. (b) Jiang, B.; Yang, S. W.; Bailey, S. L.; Hermans, L. G.; Niver, R. A.; Bolcar, M. A.; Jones, W. E. *Coord. Chem. Rev.* **1998**, *171*, 365. (c) Tour, J. M.; Kozaki, M.; Seminario, J. M. *J. Am. Chem. Soc.* **1998**, *120*, 8486. (d) Davies, W. B.; Svec, W. A.; Ratner, M. A.; Wasielewski, M. R. *Nature* **1998**, *396*, 60. (e) Creager, S.; Yu, C. J.; Bamdad, C.; O'Connor, S.; MacLean, T.; Lam, E.; Chong, Y.; Olsen, G. T.; Luo, J.; Gozin, M.; Kayyem, J. F. *J. Am. Chem. Soc.* **1999**, *121*, 1059.

(7) (a) Creutz, C. *Prog. Inorg. Chem.* **1983**, *30*, 1. (b) Richardson, D. E.; Taube, H. *Coord. Chem. Rev.* **1984**, *60*, 107.

(8) (a) Hush, N. S. *Electrochim. Acta* **1968**, *13*, 1005. (b) Hush, N. S. *Coord. Chem. Rev.* **1985**, *64*, 135.

(9) Robin, M.; Day, P. *Adv. Inorg. Radiochem.* **1967**, *10*, 247.

(10) Demadis, K. D.; Neyhart, G. A.; Kober, E. M.; Meyer, T. J. *J. Am. Chem. Soc.* **1998**, *120*, 7121.
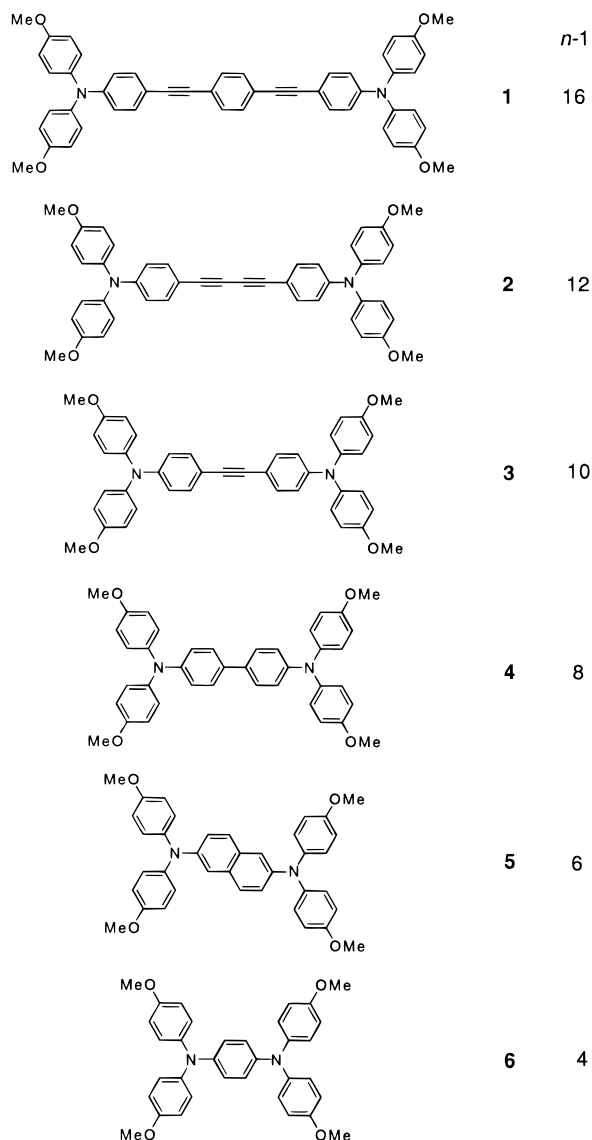
(11) Demadis, K. D.; El-Samanody, E.-S.; Coia, G. M.; Meyer, T. J. *J. Am. Chem. Soc.* **1999**, *121*, 535.

(12) (a) Ito, T.; Hamaguchi, T.; Nagino, H.; Yamaguchi, T.; Washington, J.; Kubiak, C. P. *Science* **1997**, *277*, 660. (b) Ito, T.; Hamaguchi, T.; Nagino, H.; Yamaguchi, T.; Kido, H.; Zavarine, I. S.; Richmond, T.; Washington, J.; Kubiak, C. P. *J. Am. Chem. Soc.* **1999**, *121*, 4625.

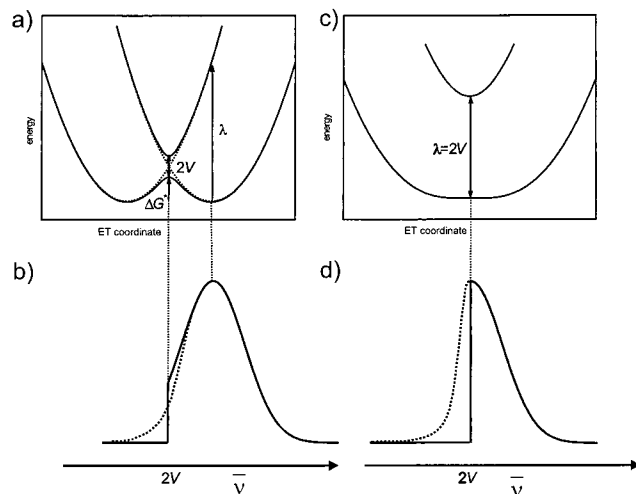(13) Marcus, R. A.; Sutin, N. *Biochim. Biophys. Acta* **1985**, *811*, 265.

(14) (a) Sutin, N. *Prog. Inorg. Chem.* **1983**, *30*, 441. (b) Creutz, C.; Newton, M. D.; Sutin, N. *J. Photochem. Photobiol. A* **1994**, *82*, 47.

Chart 1

Figure 1. (a) Potential energy diagram for $2V < \lambda$: adiabatic surfaces (solid lines); diabatic surfaces (dotted lines). (b) Theoretical Gaussian-type IV−CT absorption band shape (solid line) with cutoff at $2V$ and estimated band shape (dotted line) for the potential surfaces in a. (c) Potential energy diagram for $2V = \lambda$: adiabatic surfaces (solid lines). (d) Theoretical Gaussian-type IV−CT absorption band shape with cutoff at $2V$ (solid line) and estimated band shape (dotted line) for the potential surfaces in c.

from the IV−CT band maximum and shape. For this purpose eq 1 often is used where $\tilde{\nu}_{max}$ is the band energy in cm^{-1}, $\tilde{\nu}_{1/2}$ is the bandwidth at half-height in cm^{-1}, ϵ is the molar absorptivity, and r in Å is taken as the distance between the interacting redox centers. If the vibrational levels are in the order of k_BT or smaller, the situation relates to the high-temperature limit (HTL) and the bandwidth at 298 K is given by eq 2.

$$V = \frac{0.0206}{r}\sqrt{\tilde{\nu}_{max}\tilde{\nu}_{1/2}\epsilon} \qquad (1)$$

$$\tilde{\nu}_{1/2}(\text{HTL}) = 47.94\sqrt{\tilde{\nu}_{max}} \qquad (2)$$

$$V = \frac{\mu_{eg}}{er}\tilde{\nu}_{max} \qquad (3)$$

two parabolas and, thus, to two adiabatic surfaces where the splitting at the (avoided) intersection is twice the electronic coupling matrix element (V) of a 2×2 secular equation. Two electron-transfer pathways are conceivable: (1) the thermal process where the system moves from one minimum of the lower adiabatic surface over a transition state along the electron-transfer coordinate to the other minimum and (2) the optical way where the system is photoexcited from one minimum of the lower adiabatic surface to the Franck−Condon state of the upper adiabatic surface. The energy of this IV−CT excitation is the Marcus reorganization energy λ which comprises an inner (vibronic) part λ_v and a solvent contribution λ_s. The Hush theory[8] for analyzing IV−CT absorptions is an essentially classical theory, which is well applicable to adiabatic cases where $V \gg k_BT$. The vibrational levels are assumed to be close in energy, and the population of the vibrational levels of the ground state is weighted by a Boltzmann distribution;[15] if the diabatic potential surfaces are true parabolas, this leads to an absorption spectrum with exact Gaussian shape and $\tilde{\nu}_{max} = \lambda$. This IV−CT absorption is usually observed in the NIR. According to Hush one can deduce the electronic coupling integral V (in cm^{-1})

Equation 1 only is valid for true Gaussian-shaped curves. A more rigorous quantum chemical formulation of eq 1 is eq 3.[14b,16] In this equation μ_{eg} is the transition moment connecting the ground and the excited state, $\tilde{\nu}_{max}$ is the transition energy, and r is the distance between the diabatic (noninteracting) redox centers (e is the elementary charge). This equation has the advantage that no implicit assumption is made about the band shape as μ_{eg} (in D) can be calculated from the integrated absorbance of any band envelope via eq 4. It is not long ago

$$\mu_{eg} = 0.09584\sqrt{\frac{\int \epsilon(\tilde{\nu})d\tilde{\nu}}{\tilde{\nu}_{max}}} \qquad (4)$$

that the true nature of the pyrazine Creutz-Taube salt [(NH$_3$)$_5$-Ru-pz-Ru(NH$_3$)$_5$]$^{5+}$ was obscure;[17] finally, the IV−CT band was found in the IR and successfully modeled using vibronic coupling theory.[18] It is now commonly accepted that [(NH$_3$)$_5$-Ru-pz-Ru(NH$_3$)$_5$]$^{5+}$ is a delocalized class III compound. Prob-

(15) Nelsen, S. F.; Ismagilov, R. F.; Trieber, D. A. *Science* **1997**, *278*, 846.

(16) (a) Cave, R. J.; Newton, M. D. *Chem. Phys. Lett.* **1996**, *249*, 15. (b) Matyushov, D. V.; Ladanyi, B. M. *J. Phys. Chem. A* **1998**, *102*, 5027. (c) Newton, M. D. *Adv. Chem. Phys.* **1999**, *106*, 303.
(17) Crutchley, R. J. *Adv. Inorg. Chem.* **1994**, *41*, 273.
(18) Piepho, S. B. *J. Am. Chem. Soc.* **1990**, *112*, 4197.

lems in the interpretation arose because the IV−CT band is very weak. This is often encountered for inorganic compounds; additionally, in cases where low-lying excited $d \rightarrow$ d and MLCT or LMCT states are present, strong overlap with the IV−CT band may occur. Therefore, correct band assignments and band shape analyses are hampered; the distinction between class II and class III derivatives is often based on the bandwidth at half-height compared to the one at HTL. If the bandwidth is equal to or broader than the HTL value, the electronic situation is regarded as class II; if the bandwidth is smaller, the derivative is class III.[7a,17] However, it seems desirable to make a closer inspection of the change of band shape if a system transforms from class II to III.

In contrast to inorganic and organometallic mixed-valence compounds,[7a,17] much less is known about purely organic mixed-valence systems,[19] although a great number of derivatives have been synthesized that might have mixed-valence character in one possible oxidation state.[20] Recently, we have shown in a preliminary study that purely organic mixed-valence compounds based on triarylamines have several advantages to elucidate questions such as the one posed above:[21] triarylamines are reversibly oxidizable, the IV−CT bands are rather intense, *and* they are well separated from other bands so as to allow an accurate band shape analysis. As the inner reorganization energy is rather small (about $^{1}/_{4}$ of the total reorganization energy for acetylene-bridged triarylamines), the difference between *V* derived from optical and from thermal electron-transfer vanishes.[22] The general interest in triarylamines stems from the fact that they are widely used as hole transport components in organic optoelectronic devices such as photoconductors, photorefractive materials, or organic light-emitting devices.[23] These features make triarylamine systems an almost ideal tool kit to study electron-transfer processes and prompted us to use bistriarylamine systems with varying N−N distances in order to address the above stated question.

(19) (a) Mazur, S.; Sreekumar, C.; Schroeder, A. H. *J. Am. Chem. Soc.* **1976**, *98*, 6713. (b) Schroeder, A. H.; Mazur, S. *J. Am. Chem. Soc.* **1978**, *100*, 7339. (c) Jozefiak, T. H.; Almlöf, J. E.; Feyereisen, M. W.; Miller, L. L. *J. Am. Chem. Soc.* **1989**, *111*, 4105. (d) Rak, S. F. R.; Miller, L. L. *J. Am. Chem. Soc.* **1992**, *114*, 1388. (e) Nelsen, S. F.; Chang, H.; Wolff, J. J.; Adamus, J. *J. Am. Chem. Soc.* **1993**, *115*, 12276. (f) Bonvoisin, J.; Launay, J.-P.; Van der Auweraer, M.; De Schryver, F. C. *J. Phys. Chem.* **1994**, *98*, 5052; see correction *J. Phys. Chem.* **1996**, *100*, 18006. (g) Bonvoisin, J.; Launay, J.-P.; Rovira, C.; Veciana, J. *Angew. Chem.* **1994**, *33*, 2106. (h) Nelsen. S. F.; Adamus, J.; Wolff, J. J. *J. Am. Chem. Soc.* **1994**, *116*, 1589. (i) Lahlil, K.; Moradpour, A.; Bowlas, C.; Menou, F.; Cassoux, P.; Bonvoisin, J.; Launay, J.-P.; Dive, G.; Dehareng, D. *J. Am. Chem. Soc.* **1995**, *117*, 9995. (j) Bonvoisin, J.; Launay, J.-P.; Verbouwe, W.; Van der Auweraer, M.; De Schryver, F. C. *J. Phys. Chem.* **1996**, *100*, 17079. (k) Nelsen, S. F.; Ismagilov, R. F.; Powell, D. R. *J. Am. Chem. Soc.* **1996**, *118*, 6313. (l) Nelsen, S. F.; Ramm, M. T.; Wolff, J. J.; Powell, D. R. *J. Am. Chem. Soc.* **1997**, *119*, 6863. (m) Nelsen, S. F.; Trieber, D. A.; Wolff, J. J.; Powell, D. R.; Rogers-Crowley, S. *J. Am. Chem. Soc.* **1997**, *119*, 6873. (n) Nelsen, S. F.; Ismagilov, R. F.; Powell, D. R. *J. Am. Chem. Soc.* **1997**, *119*, 10213. (o) Nelsen, S. F.; Ismagilov, R. F.; Teki, Y. *J. Am. Chem. Soc.* **1998**, *120*, 2200. (p) Nelsen, S. F.; Ismagilov, R. F.; Powell, D. R. *J. Am. Chem. Soc.* **1998**, *120*, 1924. (q) Nelsen, S. F.; Tran, H. Q.; Nagy, M. A. *J. Am. Chem. Soc.* **1998**, *120*, 298. (r) Lambert, C.; Gaschler, W.; Schmälzlin, E.; Meerholz, K.; Bräuchle, C. *J. Chem. Soc., Perkin Trans. 2*, **1999**, 577.

(20) (a) Hünig, S.; Berneth, H. *Top. Curr. Chem.* **1980**, *92*, 1. (b) Hünig, S. *Pure Appl. Chem.* **1990**, *62*, 395.

(21) Lambert, C.; Nöll, G. *Angew. Chem., Int. Ed. Engl.* **1998**, *37*, 2107.

(22) Elliott, C. M.; Derr, D. L.; Matyushov, D. V.; Newton, M. D. *J. Am. Chem. Soc.* **1998**, *120*, 11714.

(23) (a) Stolka, M.; Yanus, J. F.; Pai, D. M. *J. Phys. Chem.* **1984**, *88*, 4707. (b) Pai, D. M.; Yanus, J. F.; Stolka, M. *J. Phys. Chem.* **1984**, *88*, 4714. (c) Borsenberger, P. M.; Weiss, D. S. *Organic Photoreceptors for Imaging Systems*; Marcel Dekker: New York, 1993. (d) Chen, C. H.; Tang, C. W. *Macromol. Symp.* **1997**, *125*, 1. (e) Katsuma, K.; Shirota, Y. *Adv. Mater.* **1998**, *10*, 223. (f) Thelakkat, M.; Schmidt, H.-W. *Adv. Mater.* **1998**, *10*, 219. (g) Selby, T. D.; Blackstock, S. C. *J. Am. Chem. Soc.* **1998**, *120*, 12155.

Table 1. Half-wave Potentials ($E_{1/2}$ vs Fc/Fc$^+$) and Difference between the First and Second Redox Process (ΔE) of **1**−**6** from Cyclic Voltammetry at a Scan Rate of 250 mV s^{-1}

	$E_{1/2}(1)$ [mV]	$E_{1/2}(2)$ [mV]	ΔE [mV]
	CH$_2$Cl$_2$/0.1 M TBAH		
1	275	335	60
2	285	385	100
3	205	355	150
4	85	305	220
5	−25	340	365
6	−145	340	485
	DMSO/0.1 M TBAH		
2	335	415	80
3	305	420	115
4	190	330	140
5	90	320	230
6	−30	310	340

Results and Discussion

The set of molecules studied (**1**−**6**) is drawn in Chart 1. The 4-methoxy substituents were chosen so as to ensure reversible oxidation of **1**−**3**. The syntheses of **1**−**6** are described in the Experimental section and were either accomplished by palladium-catalyzed C−C or C−N cross couplings (**1**, **3**, **5** and **6**, by Hagihara[24] coupling or the method developed by Hartwig[25]) or by homo coupling under Heck[26] conditions (**4**). The butadiyne **2** was synthesized by palladium-catalyzed oxidative homo coupling of the corresponding ethynyltrimethylstannane with the solvent (nitrobenzene) as the oxidant.

The triarylamine systems show N−N distances from 19.3 to 5.6 Å; however, as pointed out by Nelsen et al.,[19q] it is not the geometric distance which is important for correlating the electronic coupling *V* with the distance of redox centers but the number of bonds *n* linking the redox centers as given in Chart 1.

Electrochemistry. All compounds drawn in Chart 1 show two reversible oxidation waves in the cyclic voltammograms (CV) in CH$_2$Cl$_2$/0.1 M tetrabutylammonium hexafluorophosphate (TBAH). For compounds with redox potential splittings less than 200 mV, ΔE was obtained by digital simulation of the CVs. As one expects, the closer the triarylamine redox centers are, the larger is the redox potential splitting ΔE of the two waves (see Table 1). For **1** the CV simulation yields a redox potential splitting of 60 mV in CH$_2$Cl$_2$, the statistical value for noninteracting centers being 35.6 mV. On the strong coupling side, compound **6** shows a splitting of 485 mV where both triarylamine centers share a common phenylene spacer. A comparable triarylamine system with closer linked nitrogen centers is not conceivable.

While the potential of the first oxidation wave decreases on going from **1** to **6**, the second process is almost constant at ~340 mV vs ferrocene/ferrocenium (Fc/Fc$^+$). A similar observation was made for the reduction potentials of diquinone and diimide systems by Rak and Miller,[19d] while a series of bis(ferrocenyl)polymethine cations shows the contrary behavior: the first oxidation occurs at almost constant potential, while the second potential increases with decreasing chain length.[6a]

Oxidations of **2**−**6** were also done in DMSO/0.1 M tetrabu-

(24) Sonogashira, K. In *Metal-Catalyzed Cross-Coupling Reactions*; Dietrich, J., Stang, P. J., Eds.; Wiley-VCH: Weinheim, Germany, 1998; p 203.

(25) Hartwig, J. F. *Angew. Chem., Int. Ed. Engl.* **1998**, *37*, 2090.

(26) Bräse, S.; de Meijere, A. In *Metal-Catalyzed Cross-Coupling Reactions*; Dietrich, J., Stang, P. J., Eds.; Wiley-VCH: Weinheim, Germany, 1998; p 99.

Table 2. Band Shape Data of the IV-CT Band of 1^+-6^+ in CH_2Cl_2/0.1 M TBAH at 298 K

|	$\tilde{\nu}_{max}$ [cm^{-1}]	ϵ [M^{-1} cm^{-1}]	$\tilde{\nu}_{1/2}$(HTL) [cm^{-1}]	$\tilde{\nu}_{1/2}$(high) [cm^{-1}][a]	$\tilde{\nu}_{1/2}$(obs) [cm^{-1}][b]	$\tilde{\nu}_{1/2}$(low) [cm^{-1}][c]	$\tilde{\nu}_{1/2}$(high)/ $\tilde{\nu}_{1/2}$(low)	$\tilde{\nu}_{1/2}$(high)/ $\tilde{\nu}_{1/2}$(HTL)
1^+	9490	4570	4670	5120[d]	5120[d]	5120[d]	1.00[d]	1.10[d]
2^+	7550	8050	4160	4880	4880	4880	1.00	1.17
3^+	6190	21850	3770	4320	3960	3600	1.20	1.15
4^+	6360	28040	3820	3750	3170	2590	1.45	0.98
5^+	7620	30110	4190	4060	3210	2350	1.73	0.97
6^+	9530	22680	4680	4640	3640	2630	1.76	0.99

[a] Twice the bandwidth at half-height of the high-energy side. [b] Observed bandwidth at half-height. [c] Twice the bandwidth at half-height of the low-energy side. [d] Only $\tilde{\nu}_{1/2}$(low) could be determined; $\tilde{\nu}_{1/2}$(high) and $\tilde{\nu}_{1/2}$(obs) are assumed to be the same as $\tilde{\nu}_{1/2}$(low).

tylammonium hexafluorophosphate solutions.[27] The trend is essentially the same (Table 1) as in CH_2Cl_2; however, the potential splittings of the two oxidative processes are distinctly smaller, which can be attributed to the higher permittivity of the solvent weakening the electrostatic interaction in the dications. A correlation of $\ln(\Delta E)$ from both the CH_2Cl_2 measurements and the DMSO values vs the number of bonds $n-1$ is linear (not depicted), indicating that the splitting within a series of related compounds can be used as a measure for the electronic coupling (see section Electronic Coupling). Such a simple correlation is not usually expected and might be absent for a series of stronger differing compounds.

Spectroelectrochemistry. The UV/vis/NIR spectral changes of the triarylamine series $1-6$ upon oxidation to the mono- and to the dication were investigated in CH_2Cl_2 and DMSO by using an optical transparent thin-layer cell in a spectroelectrochemical setup described in ref 28. For all compounds a broad and rather intense absorption band rises at ~6000−10000 cm^{-1} upon oxidation to the monoradical cation. This band is assigned to the IV−CT excitation associated with a photoexcited electron transfer from a neutral triphenylamine center to the triphenyl-amine radical cation center; the band disappears when the radical species are further oxidized to the dications. The IV−CT bands of 1^+-6^+ are much more intense (ϵ ~0.5−3 × 10^4 M^{-1} cm^{-1}) than those of inorganic mixed-valence species (ϵ ~10−5000 M^{-1} cm^{-1}).[7a] For $1-3$ a very intense band at ~13000 cm^{-1} appears for the monocation, which is assigned to a $\pi-\pi^*$ excitation of the localized triphenylamine radical cation (see Figure 2a for 2^+ and 2^{2+}).[29] Accordingly, this band steadily rises when 1^+-3^+ are further oxidized to the dications. For 4^+-6^+ the corresponding radical band is much weaker and shifted to higher energy (15000−17000 cm^{-1}) (see Figure 2b for 6^+ and 6^{2+}). When oxidized to the dication, the radical band intensity at ~13000 cm^{-1} increases strongly for $4^{2+}-6^{2+}$. The spectral data for the IV−CT bands are collected in Table 2.[30]

What is expected for the IV−CT band shape if the electronic coupling V increases? We consider the adiabatic potential surfaces in Figure 1a for intermediate electronic coupling: if the lower surface is rather shallow and ΔG^* is small (this is the case when V gradually approaches $\lambda/2$) the vibrational states up to the energy of the ET transition state are significantly populated; the smallest vertical excitation energy possible is $2V$ just at the transition state. This means that, at this energy, a
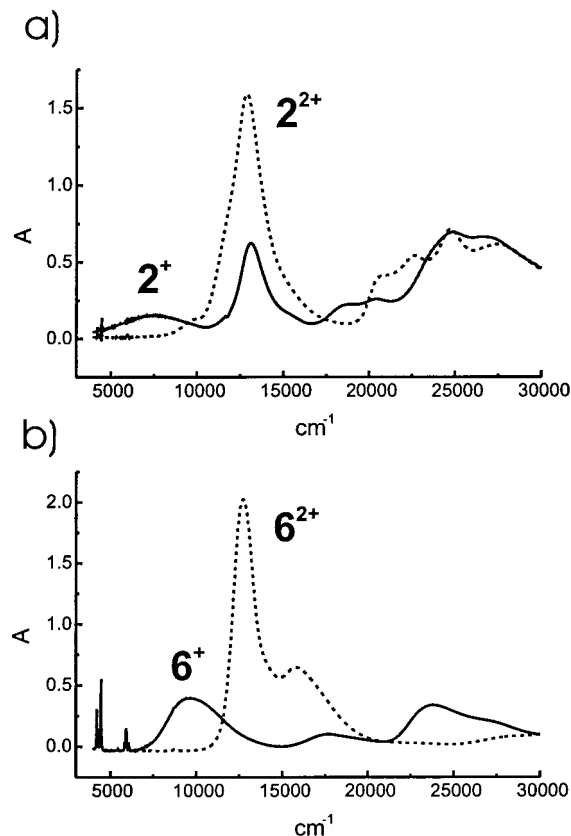
Figure 2. UV/Vis/NIR spectra of radical cations (solid lines) and dications (dotted lines) in CH_2Cl_2/0.1 M TBAH: (a) $2^+/2^{2+}$; (b) $6^+/6^{2+}$. The sharp signals below ~6000 cm^{-1} are due to the solvent.

Gaussian-shaped absorption curve is cut off (see Figure 1b).[31] Of course, an absorption band observed in practice will not be cut off sharply, but as the band envelope consists of many Gaussian-shaped sub-bands according to the vibrational fine structure, those sub-bands up to the energy of $2V$ will vanish and the band envelope falls off smoothly at the low-energy side (dotted line in Figure 1b) with a distinctly smaller bandwidth than the HTL limit. The high-energy side has the shape of the theoretical band: a Gaussian curve with a bandwidth at half-height somewhat broader or equal to the value given by eq 2 at the HTL. The point when a class II derivative transforms to a class III system is characterized by a vanishing barrier ΔG^* and by the fact that $\tilde{\nu}_{max}$ is given by $\tilde{\nu}_{max} = 2V = \lambda$ (Figure 1c).[19q] When V further increases, $\tilde{\nu}_{max}$ refers to $2V$ but it is no longer a measure for λ. This means that, at the class II/III transition, the minimum excitation energy is $2V$ and that the resulting absorption spectrum looks like the high-energy half of the theoretical Gaussian band shape at the HTL (Figure 1d).
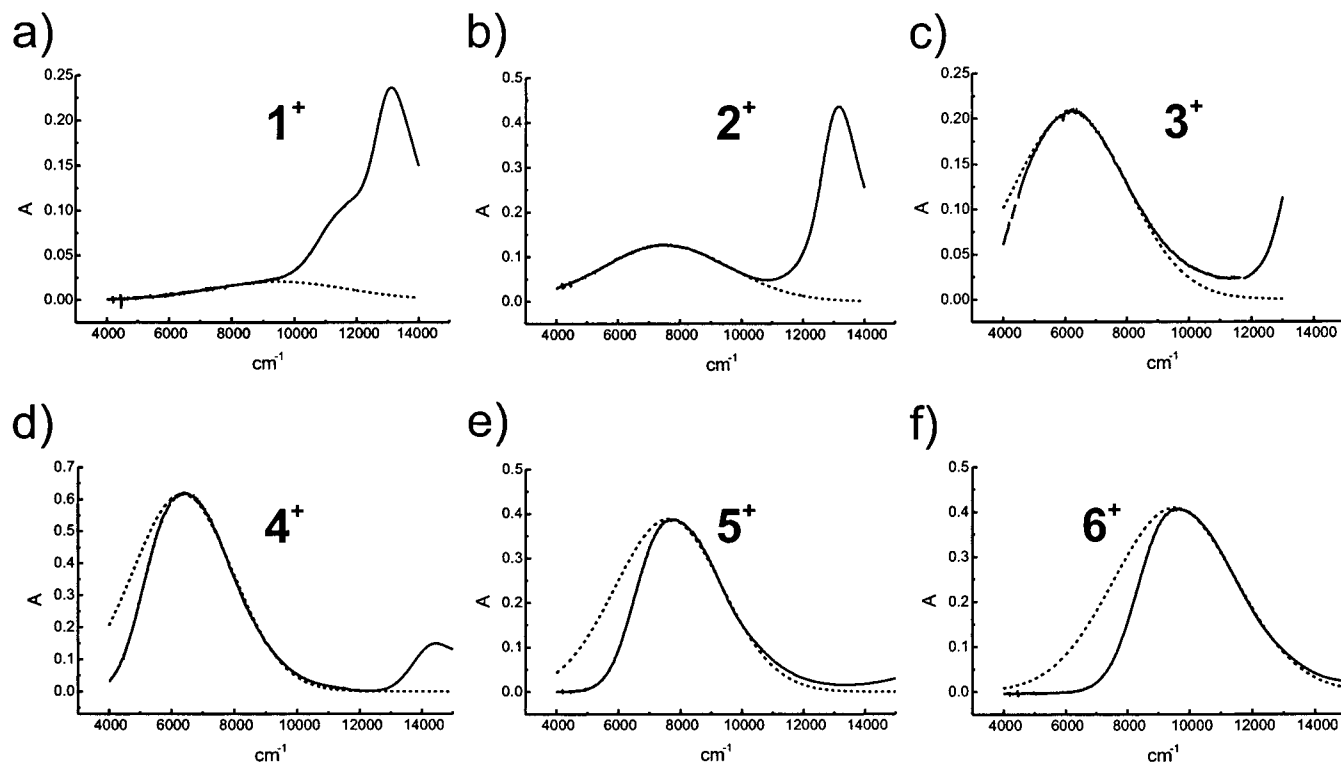
(27) The redox potentials of **1** are too close to the accessible electro-chemical window of DMSO to allow accurate measurements.

(28) Salbeck, J. *Anal. Chem.* **1993**, *65*, 2169.

(29) (a) Neugebauer, F. A.; Bamberger, S.; Groh, W. R. *Chem. Ber.* **1975**, *108*, 2406. (b) Schmidt, W.; Steckhan, E. *Chem. Ber.* **1980**, *113*, 577. (c) Dapperheld, S.; Steckhan, E.; Grosse Brinkhaus, K.-H.; Esch, T. *Chem. Ber.* **1991**, *124*, 2557.

(30) Electrochemical and spectroelectrochemical data for the related tetraphenyl-*p*-phenylenediamine radical cation can be found in (a) Cauquis, G.; Serve, D. *Anal. Chem.* **1972**, *44*, 2222. (b) Moll, T.; Heinze, *J. Synth. Metals* **1993**, *55−57*, 1521.

(31) We are especially grateful to Prof. S. Nelsen, who disvovered this aspect parallel to us, for a thorough and enlightening discussion on this point.

Figure 3. IV−CT bands of 1^+−6^+ (solid lines) from spectroelectrochemistry in CH_2Cl_2/0.1 M TBAH and Gaussian band fits (dotted lines).

Again, in practice, the band at the low-energy side will not fall off sharply but will have a very small bandwidth.

The NIR spectra for 1^+−6^+ measured by spectroelectrochemistry are given in Figure 3. The IV−CT bands for 2^+−6^+ are well separated from the adjacent radical bands, which allows accurate band fits. The spectra used for the band fits are not those of the highest absorbance of the IV−CT band of 1^+−5^+ during the electrochemical oxidation but at a point somewhat below the maximal conversion to M^+ in order to minimize overlap with bands of the dications. However, the molar absorptivities were taken from the highest IV−CT bands and are corrected for the comproportionation equilibrium as the concentration of $[M^+]$ at the highest IV−CT absorption is given by $[M^+] = [M^+]_0\sqrt{K_{co}}/(2 + \sqrt{K_{co}})$, where $[M^+]_0 = [M]_0$ is the initial and final concentration of M and of M^+, respectively, and with $K_{co} = 10^{(\Delta E/0.059)}$ where ΔE is the redox potential splitting in V.

For fitting the NIR spectra we used one Gaussian function for the IV−CT band and two functions for the adjacent radical band (the latter are not fully shown in Figure 3). The band shape analysis of the IV−CT band of 2^+ with one Gaussian function (Figure 3b) yields an almost ideal agreement. There has been much debate in the literature about the theoretical shape of a IV−CT band. Purely Gaussian functions were assumed for ϵ-$(\tilde{v})$[8] as well as for $\epsilon(\tilde{v})\tilde{v}^{32}$ or $\epsilon(\tilde{v})/\tilde{v}$.[33] Recently, Nelsen et al. suggested a quartic augmentation of the diabatic surfaces, which results in asymmetric absorption bands, that is, broader at the high-energy side and narrower at the low-energy side.[19n] However, these authors pointed out that it is not essential which type of function is used for modeling the diabatic potential surfaces but only that the result fits the experimental band.[15]

(32) Gould, I. R.; Noukakis, D.; Gomez-Jahn, L.; Young, R. H.; Goodman, J. L.; Farid, S. *Chem. Phys.* **1993**, *176*, 439. These authors showed that $\epsilon\tilde{v}$ should have Gaussian shape for absorption spectra and $\epsilon/\tilde{v}$ should have Gaussian shape for emission spectra.
(33) (a) Reimers, J. R.; Hush, N. S. *Inorg. Chem.* **1990**, *29*, 3686. (b) Reimers, J. R.; Hush, N. S. *Inorg. Chem.* **1990**, *29*, 4510.

Table 3. Hush Coupling Energy V, Thermal ET Barrier, and Rate Constant for 1^+−6^+ in CH_2Cl_2/0.1 M TBAH at 298 K

	$r = d_{NN}$ [Å]	$n - 1$	μ_{eg} [D]	V [cm^{-1}]	ΔG^* [cm^{-1}]	k_{th} [s^{-1}]
1^+	19.30	16	4.89	500	1900	9.3×10^8
2^+	15.02	12	6.39	710	1280	1.9×10^{10}
3^+	12.48	10	11.6	1200	580	5.5×10^{11}
4^+	9.93	8	11.6	1550	420	1.2×10^{12}
5^+	7.86	6	11.1	2240	320	1.9×10^{12}
6^+	5.62	4	9.17	3240	240	2.8×10^{12}

Thus, we further assume that the high-energy side of the IV−CT band of 1^+ and 3^+−6^+ can be simulated with a single Gaussian function analogously to 2^+. The IV−CT bandwidth at half-height of 2^+ is somewhat broader[34] than the theoretical value at the HTL (eq 2), which proves 2^+ to be a valence-trapped class II derivative. The electronic coupling V was evaluated to be 710 cm^{-1} using eq 3 and the values given in Tables 2 and 3. For r we used the N−N distance from an AM1-UHF optimization (see Introduction) and μ_{eg} was calculated with eq 4 and the integrated IV−CT band (taken as the area under the Gaussian fit curve). The IV−CT band of 1^+ shows strong overlap with a shoulder of the radical band. Thus, for the band fit, a symmetric Gaussian-shaped curve was assumed. The IV−CT bands of 3^+−6^+ are apparently asymmetric (Figure 3c−f). Thus, for the Gaussian fit we used only the high-energy side of the IV−CT band (one function) and the adjacent radical bands (two functions). For the evaluation of μ_{eg}, we used the area under the IV−CT band minus those parts belonging to the radical band. The value $\tilde{v}_{max}$ in Table 1 is not the energy at maximal absorption of the IV−CT band but the one of the Gaussian fit which is at marginally lower energy.

(34) Assuming parabolic diabatic potentials for 2^+, one gets a Gaussian-shaped band with $\tilde{v}_{1/2}$(HTL) that is narrower than the observed one (see Table 2). Prof. S. Nelsen (private communication) pointed out that using quartic augmented diabatic functions[19n] would give an asymmetric band shape for 2^+ but with the correct observed bandwidth. A consequence is that λ is no longer $\tilde{v}_{max}$. This results in a ΔG^* that is $\sim$10% smaller than the one given in Table 3. Thus, the ΔG^* values in Table 3 may be regarded as upper bounds.

It can easily be seen that the Gaussian curve fits well to the high-energy side of the IV−CT band of 3^+−6^+ but that the low-energy side distinctly narrows the closer the nitrogen centers are linked. This behavior has been anticipated by the Hush theory (see above) and reflects the cutoff at $2V$ at the low-energy side of the IV−CT band when the coupling V approaches $\lambda/2$. The ratio of the bandwidth at half-height of the high-energy side and the one of the low-energy side is taken as a measure for the asymmetry; it increases steadily from 1.00 to 1.76 on going from 1^+ to 6^+ (see Table 2). For 1^+−3^+ the bandwidth at half-height of the high-energy side is somewhat broader than the HTL limit, which is consistent with a class II system.[8] For 4^+−6^+ the bandwidth of the high-energy side is within experimental error that of the HTL limit (eq 2).

Electronic Coupling. By using the data from Table 2 and eq 3, we calculated the electronic coupling integral V for 1^+−6^+. At this point we have to make a statement about the electron-transfer distance r used in eqs 1 and 3. While usually taken as the metal−metal distance in inorganic mixed-valence systems, recent publications try to evaluate the "true" electron-transfer distance in some inorganic binuclear compounds and of some purely organic bishydrazine mixed-valence compounds: the quantity $\Delta\mu = er$ was determined by either electrooptic absorption measurements (Stark spectroscopy) of the change of dipole moment upon photoinduced electron transfer[35] or via semiempirical calculations of this quantity as twice the ground-state dipole moment.[36] Alternatively, the dipolar splitting of phenylenedihydrazine triplet dications was used to derive r.[19n] All of these studies indicate the effective electron-transfer distance to be smaller than the metal−metal or nitrogen−nitrogen distance. Some extent of ground-state delocalization or charge flow from the ligands was assumed as the reason for the smaller distance. However, as outlined in ref 14b and 16, the distance r in eqs 1 and 3 is *not* defined by $\Delta\mu = er$, where $\Delta\mu$ is the difference of dipole moment of the *adiabatic* states but is defined as $r = (\mu_a - \mu_b)/e$, where μ_a and μ_b are the dipole moments of the *localized diabatic* (noninteracting) states. In these states there is no ground-state delocalization between the redox centers, and the assumption that the average position of the electron transferred is that of the metal center or that of a nitrogen position (in the compounds studied in this paper) is probably more accurate than evaluating r from $\Delta\mu$. This assumption will be more accurate the less the local asymmetry of the redox centers is. As one can expect a fairly symmetric local electron distribution in triarylamine radical cations, we will retain to use the nitrogen−nitrogen distance for r in what follows.[37,38]

(35) Bublitz, G. U.; Laidlaw, W. M.; Denning, R. G.; Boxer, S. G. *J. Am. Chem. Soc.* **1998**, *120*, 6068.

(36) Nelsen, S. F. private communication.

(37) According to ref 16a, one can calculate the difference of the diabatic dipole moments from the difference of the adiabatic dipole moments and the transition moment: $\mu_a - \mu_b = \sqrt{\Delta\mu^2 + 4\mu_{eg}^2}$. In principle these adiabatic quantities can be determined experimentally; however, for the series of ions studied in this paper, there are no experimental dipole moments available. Using $\Delta\mu$ as twice the AM1-calculated dipole moment $\mu_{g,calc}$ and the experimental transition moment μ_{eg} from Tables 3 and 4, we calculated $r = (\mu_a - \mu_b)/e$ for 1^+−6^+: 1^+ 17.21, 2^+ 12.82, 3^+ 11.26, 4^+ 9.31, 5^+ 7.22, 6^+ 3.98 Å. These distances are somewhat shorter than d_{NN} for 1^+−5^+ and would increase V by a factor of 1.07−1.17. However, for 6^+ this factor is 1.47, which makes $V(6^+) = \tilde{\nu}_{max}/2$. As we do not know how accurate the calculations of μ_g of 1^+−6^+ are and we do not want to mix up experimental and calculated quantities for the evaluation of V, we use $r = d_{NN}$ in the present paper.

(38) In fact, ESR spectroscopic investigations of triarylamines show that $2/3$ of the spin density is delocalized in the phenyl rings and $1/3$ is localized at the nitrogen (see ref 29a). Thus, the N−N distance in 1^+−6^+ merely represents a mean ET distance.
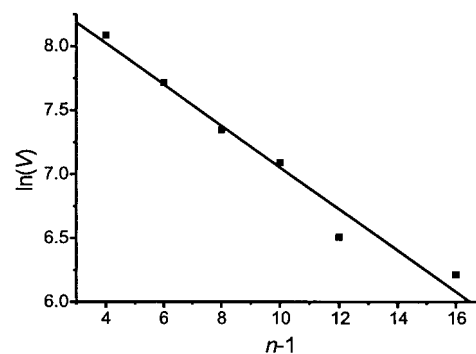
Figure 4. Correlation of ln(V) vs bond link $n − 1$ for 1^+−6^+.

The results for V using the nitrogen−nitrogen distance, r, are given in Table 3 and span a range from 500 cm^{-1} (1^+) to 3240 cm^{-1} (6^+). For 6^+, $\lambda/2 = 4765$ cm^{-1}, which shows that the tetra(4-methoxyphenyl)phenylenediamine 6^+ is still a class II compound just at the borderline to class III when $V = \lambda/2$. This contrasts the behavior of tetramethylphenylenediamine radical cation (Wurster's blue), which clearly is a class III system with vibrational splitting of the IV−CT band.[3a,39] The electronic couplings found for 1^+−6^+ are much stronger than those of inorganic mixed-valence compounds ($V \sim 10-1000$ cm^{-1}).[7a]

For the case of an ET via a super exchange mechanism,[40] one expects an exponential decay of V with the ET distance $n − 1$ (see eq 5).[5,6d,19q] Although 1^+−6^+ is not a true homologous series and conformational distributions in 1^+−4^+ were neglected,[41] a good ($R = 0.985$) linear correlation of ln(V) vs $n − 1$ is observed with a β value of 0.32 and $V_0 = 5825$ cm^{-1} (Figure 4). Similar β values have been evaluated for olefin-bridged ruthenium and dialkylamino compounds.[42] The linear correlation supports our interpretation that 6^+ still is a class II compound since otherwise V should be $\lambda/2 = 4765$ cm^{-1} and the data point for 6^+ would lie too high in the plot (Figure 4).

$$V = V_0 e^{(-\beta(n-1)/2)} \tag{5}$$

A correlation of the redox potential splitting ΔE in CH$_2$Cl$_2$ vs the electronic coupling V is linear as can be seen in Figure 5. Although the redox potential splitting ΔE refers to the interaction of the redox centers in the vibrationally relaxed dication, it can be used as a rough guide for the electronic coupling V in the monocation.[19e] The magnitude of the comproportionation constant (K_{co}) is often taken as an indicator for strong or weak coupling.[7,17] However, this is, to the best of our knowledge, the first time that such a linear correlation of ΔE vs V was observed over almost one order of magnitude.[43] We suppose that the correlation works well in the present case because the structural reorganization between neutral and cationic species on one hand and between cation and dication on the other hand is not affected by each other. One expects larger deviations when, for example, a second oxidation (or reduction) of a species is made easier by a major structural reorganization already

(39) (a) Meyer, W. C.; Albretch, A. C. *J. Phys. Chem.* **1962**, *66*, 1168. (b) Nelsen, S. F.; Yunta, M. J. R. *J. Phys. Org. Chem.* **1994**, *7*, 55. In principle, one should not speak of IV−CT bands in delocalized class III systems where neither charge is transferred nor two different valences are present. Although incorrect, we retain using this term because of the lack of a better one.

(40) Kosloff, R.; Ratner, M. A. *Isr. J. Chem.* **1990**, *30*, 45.

(41) Sachs, S. B.; Dudek, S. P.; Hsung, R. P.; Sita, L. R.; Smalley, J. F.; Newton, M. D.; Feldberg, S. W.; Chidsey, C. E. D. *J. Am. Chem. Soc.* **1997**, *119*, 10563.

(42) See ref 19q where values from ref 33a were used for obtaining β.
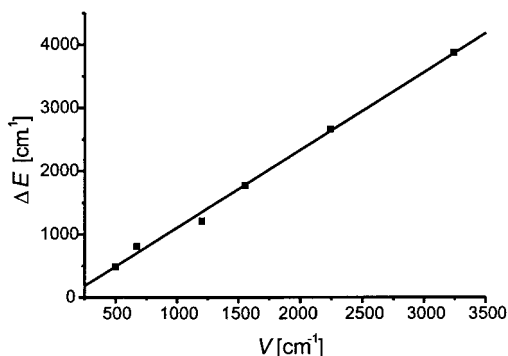
Figure 5. Correlation of redox potential splitting ΔE (in cm^{-1}) vs electronic coupling V for 1^+–6^+.

expended in the first oxidation (reduction) step.[44] It is interesting to note that, according to the linear correlation (Figure 5), when ΔE approaches the statistical value of 35.6 mV (287 cm^{-1}) for noninteracting redox centers, V does not vanish but is still 340 $\pm$ 55 cm^{-1}. This deviation seems not to be within experimental error and might be due to ion-pairing effects.[19e,45] It actually means that there is an offset of about -50 mV for observing electronic coupling by cyclic voltammetry in the systems studied. Ion-pairing effects might also influence the slope of the correlation, which is 1.23 but should be 2.0 because the two oxidation potentials scan the relative HOMO and HOMO-1 energies whose difference would be $2V$ if electron–electron interactions were negligible (Hückel model).[46]

AM1-calculated coupling energies were derived from the energy splittings (corresponding to $2V$)[5b,19f,47] of the HOMO and HOMO-1 of the neutral species **1**–**6** as these symmetric geometries are presumably more similar to the symmetric ET transition state than the relaxed radical cation structures.[48] The AM1 calculations reproduce the experimental trend very well; however, the increase of coupling with decreasing $n-1$ is smaller than in the experiment. The value of 4^+ seems to be too small (1258 cm^{-1} vs 1270 cm^{-1} in 3^+), which might be due to the twisted biphenyl geometry (angle of the phenyl groups 38.4°) of neutral **4**.[49] If forced to be planar, the resulting HOMO/HOMO-1 splitting gives a coupling integral of 1575 cm^{-1}; this suggests that V of the radical cation transition state is somewhere between.[48] For 6^+ we also calculated V with an RHF wave

function on the UHF radical cation geometry ($V = 4747$ cm^{-1}). This value is much higher than that of the neutral geometry and is in good agreement with $\tilde{\nu}_{max}/2 = 4765$ cm^{-1} if one assumes class III behavior.[19q] For valence-trapped class II compounds, one expects a nonzero dipole moment. Although the dipole moment of ions is origin-dependent, one can calculate relative dipole moments using the center of mass as the origin. The AM1-UHF-calculated values for 1^+–5^+ are substantial and are given in Table 4. For 6^+ the dipole moment vanishes and suggests a class III structure. This might be either an artifact of the AM1-UHF method or due to the fact that the computation refers to the gas phase while in reality the solvent induces a charge localization in 6^+.

Reorganization Energies. The internal contribution to the reorganization energy for 3^+ has been evaluated from solvent-dependent measurements of the IV–CT band energy vs the Dimroth-Reichardt solvent parameters and extrapolating the values to the gas phase where only the internal part λ_v is present.[21,50] This gives $\lambda_v = 1600$ cm^{-1} for 3^+. By using only the values for CH_2Cl_2/TBAH and DMSO/TBAH, one gets a somewhat higher value of 2100 cm^{-1}, which is still within the range of the rather crude approximation.[51] Hence, for the other derivatives 2^+ and 4^+–6^+ we used only the CH_2Cl_2 and DMSO values to estimate λ_v (see Table 4). The values obtained for 2^+ and 3^+ are in reasonable agreement with the AM1-calculated values applying the method by Nelsen et al.[52] These authors used the enthalpy change (eq 6) when the radical cation (heat of formation: c^+) is calculated in the geometry of the neutral species (n^+) and the neutral compound (n^0) is calculated in the geometry of the radical cation (c^0) as an estimate for λ_v. The values calculated in this way are collected in Table 4. For 4^+–6^+, there is an increasing deviation of the AM1 energies from the experimental values (see Figure 6); this is reasonable as this method should be only applicable in cases of relatively weak coupling.

$$\lambda_{v,calc} = c^0 - c^+ + n^+ - n^0 \qquad (6)$$

For 1^+ we were unable to determine λ in DMSO, but we are quite confident that the AM1-calculated value λ_v is correct.[27] Henceforth, we used this value for further evaluations. While $\lambda_{v,exp}$ is $\sim 1/3$ of λ for 1^+–3^+, it increases to $\sim 80\%$ of λ for 6^+. For an ideal class III system, one expects no major solvent dependence of λ as there is only internal reorganization left.

The total reorganization energy λ shows a minimum for 3^+ and 4^+ (see Figure 6) and rises to both the weak coupling regime and the strong coupling side. This curve is the result of a superposition ($\lambda = \lambda_v + \lambda_s$) of the internal and the solvent contribution, which display opposite trends. The latter (calculated as $\lambda_s = \lambda - \lambda_{v,exp}$) falls off with decreasing r on going from 1^+ to 5^+ as anticipated by the well-known eq 7. This equation was derived from a dielectric continuum model where

(43) There have been many attempts in the literature to correlate redox potential splittings with spectroscopic data, see, for example, (a) de la Rosa, R.; Chang, P. J.; Salaymeh, F.; Curtis, J. C. *Inorg. Chem.* **1985**, *24*, 4231. (b) Dong, Y.; Hupp, J. T. *Inorg. Chem.* **1992**, *31*, 3170. (c) Evans, C. E. B.; Naklicki, M. L.; Rezvani, A. R.; White, C. A.; Kondratiev, V. V.; Crutchley, R. J. *Am. Chem. Soc.* **1998**, *120*, 13096. Crutchley et al. did not find a linear correlation between electrochemically determined resonance energies and energies derived from a Hush analysis for a series of transition metal complexes. However, the complexes were studied in different solvents and were not a homologous series.

(44) Salbeck, J.; Schöberl, U.; Rapp, K. M.; Daub, J. *Z. Phys. Chem.* **1991**, *171*, 191.

(45) Nishihara, H.; Nakagawa, T.; Aramaki, K. *Electroanalysis* **1996**, *8*, 831.

(46) Lee, S. K.; Zu, Y.; Herrmann, A.; Geerts, Y.; Müllen, K.; Bard, A. J. *Am. Chem. Soc.* **1999**, *121*, 3513.

(47) Newton, M. D. *Chem. Rev.* **1991**, *91*, 767.

(48) Direct optimization of the ET transition state with the UHF method and subsequent RHF single-point calculation in principle would allow a more accurate estmate of V. However, the AM1-UHF calculation of the symmetric ET transition state of, for example, 3^+ yielded an asymmetric charge distribution even when the geometry was restricted to be symmetric. Therefore, this electronic structure is not the correct transition state on the ET coordinate. As there is no way to force the wave function to be symmetric using Mopac97, we used the geometry of the neutral species for obtaining V.

(49) For a discussion of the influence of torsional angles on the electronic coupling in biphenyl systems, see ref 19q.

(50) Nelsen, S. F.; Kim, Y.; Blackstock, S. C. *J. Am. Chem. Soc.* **1989**, *111*, 2045.

(51) From a linear correlation of λ of 3^+ vs the Dimroth-Reichardt parameters of six pure solvents and the measured value of λ in CH_2Cl_2/TBAH, we calculated a pseudo-E_T^N parameter (0.323) for CH_2Cl_2/0.1 M TBAH solution used in the spectroelectrochemical experiments. As expected, this value is slightly higher than that of pure CH_2Cl_2. With this value for CH_2Cl_2/0.1 M TBAH and the one for pure DMSO (0.444, supporting electrolyte is not expected to have a strong influence on the apparent E_T^N value in such highly polar solvents), we calculated λ_v for 2^+–6^+ using the follwing equation and the absorption maxima in CH_2Cl_2/TBAH and in DMSO/TBAH: $\lambda_v(E_T^N(DMSO)/E_T^N(CH_2Cl_2/TBAH) - 1) = \tilde{\nu}_{max}(CH_2Cl_2/TBAH)[E_T^N(DMSO)/E_T^N(CH_2Cl_2/TBAH)] - \tilde{\nu}_{max}(DMSO)$.

(52) Nelsen, S. F.; Blackstock, S. C.; Kim, Y. *J. Am. Chem. Soc.* **1987**, *109*, 677.

Table 4. AM1-Calculated Data (calc) and Solvent Dependence of $\tilde{\nu}_{max}$ for 1^+–6^+

	$\tilde{\nu}_{max} = \lambda$ [cm^{-1}] in CH$_2$Cl$_2$	$\tilde{\nu}_{max} = \lambda$ [cm^{-1}] in DMSO	$\Delta\tilde{\nu}_{max}$ [cm^{-1}]	$\lambda_{v,exp}$ [cm^{-1}]	$\lambda_s{}^a$ [cm^{-1}] in CH$_2$Cl$_2$	$\lambda_{v,calc}$ [cm^{-1}]	$V_{calc}{}^b$ [cm^{-1}]	$\mu_{g,calc}$ [D]
1^+	9490				$(6457)^c$	3033	564	41.0
2^+	7550	9300	1750	2900	4650	2808	944	30.1
3^+	6190	7740	1550	2100	4090	1575	1270	24.4
4^+	6360	7540	1180	3200	3160	2153	1258	19.1
5^+	7620	8210	590	6100	1520	3637	2038	13.3
6^+	9530	10130	600	7900	1630	5139	2429 $(4747)^d$	0.0

^{a} Calculated as $\lambda_s = \lambda - \lambda_{v,exp}$. ^{b} Calculated as $[e(\text{HOMO}) - e(\text{HOMO-1})]/2$ of 1–6. ^{c} Calculated from $\lambda_{v,calc}$. ^{d} Calculated as $[e(\text{HOMO}) - e(\text{HOMO-1})]/2$ of an RHF wave function on the UHF geometry of 6^+.
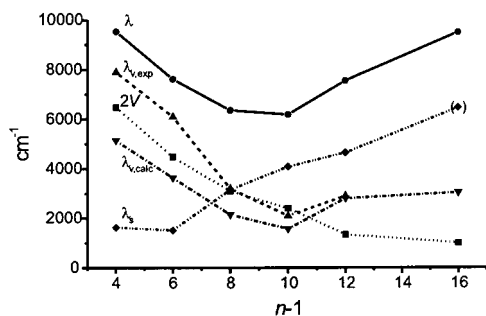
Figure 6. Correlation of the reorganization energies vs bond link $n - 1$ for 1^+–6^+. The point in parentheses was derived from $\lambda_{v,calc}$.

a and r are the radius and the distance of the redox centers, respectively, n is the index of refraction, and ϵ is the permittivity.[53]

$$\lambda_s = e^2\left(\frac{1}{a} - \frac{1}{r}\right)\left(\frac{1}{n^2} - \frac{1}{\epsilon}\right) \quad (7)$$

On the other hand, the internal reorganization λ_v rises strongly from 3^+ to 6^+. This might be due to the strong increases of V (given as $2V$ in Figure 6), although when quadratic diabatic functions are used, λ should not depend on V.[19n]

ET Rate Constants. If the electronic coupling is large compared to one-quarter of the Marcus reorganization energy λ, the thermal ET is adiabatic and the activation energy cannot be evaluated by the simple Marcus expression $\Delta G^* = \lambda/4$. Instead we used eq 8 derived by Sutin et al.,[14] which yields a lower barrier. For an adiabatic ET, tunneling factors can be ignored and eq 9 is applicable for estimating the intramolecular ET rate constants.[14a]

$$\Delta G^* = \frac{\lambda}{4} - V + \frac{V^2}{\lambda} \quad (8)$$

$$k_{th} = \nu_n e^{-(\Delta G^*/RT)} \quad (9)$$

$$g(\nu_n, T) = \left[\frac{h\nu_n}{2k_B T}\coth\frac{h\nu_n}{2k_B T}\right]^{1/2} \quad (10)$$

The nuclear frequency factor ν_n in eq 9 was estimated from the ratio g of the bandwidth of the high-energy side and the bandwidth at HTL (eq 10).[8b] Analyzing the IV–CT spectra gave $\nu_n = 300$ cm^{-1} ($= 9 \times 10^{12}$ s^{-1}) for 2^+ and 280 cm^{-1} for 3^+. Because for 4^+–6^+ there is no band broadening compared to HTL we simply assumed a value of 300 cm^{-1} for all species. This seems to be reasonable, as the AM1-UHF-optimized radical cations show only small geometric changes compared to the neutral compounds; these changes are mainly torsions of the

(53) Brunschwig, B. S.; Ehrenson, S.; Sutin, N. *J. Phys. Chem.* **1986**, *90*, 3657.

phenyl groups and should be associated with low-energy vibrations, thus justifying the assumption of the low 300 cm^{-1} value. The ET rate constants for 1^+–6^+ are given in Table 3. Even for the di(phenylethynyl)benzene derivative 1^+, the rate constant is very high (9.3×10^8 s^{-1}). For 6^+ the ET rate constant (2.8×10^{12} s^{-1}) reaches the regime of molecular vibrations and the system is at the border to be vibrationally detrapped.

Conclusions

The distances between the redox centers in the set of triarylamine compounds presented in this study span a range from a few Angstroms (6^+) to 2 nm (1^+). Despite this long separation, the redox centers even in 1^+ are rather strongly coupled ($V = 500$ cm^{-1}). This allows the observation and comparison of mixed-valence properties over a broad distance range: the total reorganization energy λ has a minimum for intermediate bond links $n - 1$ as the result of two opposing trends in λ_v and λ_s. The electronic coupling integral V was evaluated from the integrated IV–CT band absorbance and rises strongly from 1^+ to 6^+ but is smaller than $\lambda/2$ for all compounds investigated in this study. This demonstrates that even the phenylene derivative is a valence-trapped class II compound. This interpretation is supported by a linear correlation of $\ln(V)$ vs $n - 1$. For 6^+ an ET activation barrier of 240 cm^{-1} vs $\lambda = 9530$ cm^{-1} and a coupling of 3240 cm^{-1} shows that the system is just before the transition to a class III situation. The line shape analyses of the radical cation IV–CT bands of 4^+–6^+ gave a distinctly smaller bandwidth at half-height than the theoretical HTL value. This narrowing is due to a cutoff of the low-energy side of the band at $2V$, while the high-energy side follows the theoretical band shape. Henceforth, a distinction between class II and class III cannot solely be made on the basis of bandwidth because a narrow bandwidth is expected even for class II systems when $2V$ approaches λ. In theory, the narrowing of the low-energy side should be observed when $2V$ exceeds $\tilde{\nu}$ at $\epsilon_{max}/2$. Owing to the inhomogeniously broadened vibrational sub-bands, the cutoff at $2V$ is smooth and occurs earlier on the $\tilde{\nu}$ scale. Instead, for a discrimination between class II and III, the magnitude of $2V$ should be compared to λ. The relative electronic coupling can also be evaluated from redox potential splittings as there is a linear correlation.

The ET rate constants were estimated from V and indicate ultrafast ET even for the di(phenylethynyl)benzene system 1^+. The rate constants approach the time scale of molecular vibrations for 6^+. Our study shows that ET processes can be extremely fast in triarylamine multi redox center systems, which is a consequence of the strong electronic coupling compared to a rather small reorganization energy. The latter is small because the charge (spin) is partly delocalized in the triarylamine moieties.[38] Triarylamines are currently used as hole carrier components in organic optoelectronic devices. While in these materials the long-range electron or hole transfer acts by a

hopping mechanism, one can conceive of oligotriarylamine systems based on substructures studied in this paper where hole transport on a nanoscale is accomplished by ultrafast superexchange. Work on this topic is currently in progress.

Experimental Section

Syntheses. All palladium-catalyzed couplings were performed under nitrogen inert gas atmosphere in dry oxygen-free solvents.

Bis{4-[*N*,*N*-di(4-methoxyphenyl)amino]phenylethynyl}benzene 1. 1,4-Diiodobenzene (48 mg, 0.146 mmol), 4-[*N*,*N*-di(4-methoxyphenyl)-amino]phenylacetylene[54] (109 mg, 0.331 mmol), PdCl$_2$(PPh$_3$)$_2$ (20 mg, 10 mol %), and CuI (4 mg, 7 mol %) were dissolved in dry diethylamine (8 mL) and stirred at 55 °C for 6 h. The solvent was removed in vacuo, and the residue was purified by flash chromatography on silica gel (PE/CH$_2$Cl$_2$ 1:1). The crude yellow product (80 mg, 75%) contains **2** as an impurity. Flash chromatography (PE/CH$_2$Cl$_2$ 2:1) gave pure **1** in the slower running fractions (NMR control), which can be precipitated from CH$_2$Cl$_2$/MeOH. Mp: 87−90 °C. ^{1}H NMR (250 MHz, CDCl$_3$): $\delta = 7.43$ (s, 4H, phenylene), 7.29 (m, 4H, AA′, aminophenyl), 7.07 (m, 8H, AA′, 4-methoxyphenyl), 6.86 (m, 8H, BB′, 4-methoxyphenyl), 6.81 (m, 4H, BB′, aminophenyl), 3.78 (s, 12H, methoxy). ^{13}C NMR (62.9 MHz, CDCl$_3$): $\delta = 156.4$, 149.0, 140.3, 132.4, 131.2, 127.3, 123.2, 119.2, 114.9, 113.9, 91.8, 88.1, 55.5. MS (EI, 70 eV, high resolution): calcd, $m/z = 732.2988$; found, 732.2979.

Bis{4-[*N*,*N*-di(4-methoxyphenyl)amino]phenyl}butadiyne 2. 4-[*N*,*N*-di(4-methoxyphenyl)amino]phenylethynyltrimethylstannane (prepared analogously to the tributylstannane in ref 54) (175 mg, 0.356 mmol) and Pd(PPh$_3$)$_4$ (7 mg, 2 mol %) were dissolved in dry nitrobenzene (4 mL) and stirred at 80−90 °C for 4 h. The solvent was removed in vacuo and the residue purified by flash chromatography on silica gel (PE/CH$_2$Cl$_2$ 1:1). Precipitation from a CH$_2$Cl$_2$ solution with PE gave 75 mg (64%) of a yellow powder. Mp: 189−190 °C. ^{1}H NMR (250 MHz, CDCl$_3$): $\delta = 7.25$ (m, 4H, AA′, aminophenyl), 7.07 (m, 8H, AA′, 4-methoxyphenyl), 6.86 (m, 8H, BB′, 4-methoxyphenyl), 6.75 (m, 4H, BB′, aminophenyl), 3.79 (s, 12H, methoxy). ^{13}C NMR (62.9 MHz, CDCl$_3$): $\delta = 157.3$, 150.1, 140.1, 133.6, 127.9, 118.7, 115.3, 112.2, 82.5, 73.3, 55.9. Anal. calcd for C$_{44}$H$_{36}$N$_2$O$_4$ (656.78): C 80.47, H 5.52, N 4.27. Found: C 80.1, H 5.6, N 4.3.

Bis{4-[*N*,*N*-di(4-methoxyphenyl)amino]phenyl}acetylene 3. 4-[*N*,*N*-di(4-methoxyphenyl)amino]phenyacetylene[54] (500 mg, 1.52 mmol), *N*,*N*-di(4-methoxyphenyl)-4-iodophenylamine[54] (685 mg, 1.59 mmol), PdCl$_2$(PPh$_3$)$_2$ (53 mg, 5 mol %), and CuI (7 mg, 2.5 mol %) were dissolved in dry diethylamine (25 mL) and stirred at 55 °C for 6 h. The solvent was removed in vacuo, and the residue was purified by flash chromatography on silica gel (PE/CH$_2$Cl$_2$ 1:1). Precipitation from a CH$_2$Cl$_2$ solution with MeOH gave 519 mg (82%) of a yellow powder. Mp: 109−110 °C. ^{1}H NMR (250 MHz, CDCl$_3$): $\delta = 7.25$ (m, 4H, AA′, aminophenyl), 7.07 (m, 8H, AA′, 4-methoxyphenyl), 6.86 (m, 8H, BB′, 4-methoxyphenyl), 6.83 (m, 4H, BB′, aminophenyl), 3.79 (s, 12H, methoxy). ^{13}C NMR (62.9 MHz, CDCl$_3$): $\delta = 156.3$, 148.4, 140.5, 132.2, 127.4, 119.6, 114.9, 114.9, 88.6, 55.5. Anal. calcd for C$_{42}$H$_{36}$N$_2$O$_4$ (632.74): C 79.75, H 5.74, N 4.43. Found: C 79.5, H 5.8, N 4.1.

4,4′-Bis[*N*,*N*-di{4-methoxyphenyl}amino]biphenyl 4.[55] *N*,*N*-di{4-methoxyphenyl}-4-iodophenylamine[54] (200 mg, 0.464 mmol), K$_2$CO$_3$ (430 mg, 3.11 mmol), Pd(O$_2$CCH$_3$)$_2$ (7 mg, 7 mol %), and Bu$_4$NBr (1.5 g, 4.65 mmol) were dissolved in dry DMF (8 mL) and refluxed for 18 h. The solvent was removed in vacuo. The residue was purified by chromatography on alumina (N, S1, PE/CH$_2$Cl$_2$ 1:3). The crude product was precipitated twice from a CH$_2$Cl$_2$ solution with MeOH, which gave 85 mg (60%) of a yellow powder. ^{1}H NMR (250 MHz, CD$_2$Cl$_2$): $\delta = 7.35$ (m, 4H, AA′, biphenyl), 7.04 (m, 8H, AA′, 4-methoxyphenyl), 6.95−6.85 (m, br, 4H, BB′, biphenyl), 6.82 (m, 8H,

BB′, 4-methoxyphenyl), 3.78 (s, 12H, methoxy). ^{13}C NMR (62.9 MHz, CD$_2$Cl$_2$): $\delta = 156.5$, 148.0, 141.5, 133.3, 127.1, 126.9, 121.4, 115.1, 55.9.

2,6-Bis[*N*,*N*-di(4-methoxyphenyl)amino]naphthalene 5. 2,6-Dibromonaphthalene[56] (100 mg, 0.350 mmol), di(4-methoxyphenyl)amine (197 mg, 0.859 mmol), NaO^{t}Bu (120 mg, 1.25 mmol), tris-*o*-tolylphosphine (37 mg, 17 mol %), and Pd$_2$(dba)$_3$·CHCl$_3$ (31 mg, 4 mol %) were dissolved in dry *p*-xylene (6 mL) and stirred at 90−100 °C for 5 h. The solvent was removed in vacuo, and the residue was purified by flash chromatography on silica gel (PE/CH$_2$Cl$_2$ gradient 1:1−1:∞). The product was precipitated from a CH$_2$Cl$_2$ solution with MeOH to give 109 mg (53%) of a yellow powder. Mp: 220−221 °C. ^{1}H NMR (250 MHz, CDCl$_3$): $\delta = 7.37$ (m, br, 2H, napht.), 7.09 (m, 8H, AA′, 4-methoxyphenyl), 7.03 (br, 4H, napht.), 6.81 (m, 8H, BB′, 4-methoxyphenyl), 3.79 (s, 12H, methoxy). ^{13}C NMR (62.9 MHz, CDCl$_3$): $\delta = 155.6$, 144.9, 141.2, 130.3, 127.4, 126.0, 123.6, 117.6, 114.7, 55.5. MS (EI, 70 eV, high resolution): calcd, $m/z = 582.25189$; found, 582.25111.

***N*,*N*,*N*′,*N*′-Tetra(4-methoxyphenyl)-1,4-phenylenediamine 6.**[23g] 1,4-Dibromobenzene (81 mg, 0.344 mmol), di(4-methoxyphenyl)amine (197 mg, 0.859 mmol), NaO^{t}Bu (120 mg, 1.25 mmol), tris-*o*-tolylphosphine (37 mg, 17 mol %), and Pd$_2$(dba)$_3$·CHCl$_3$ (31 mg, 4 mol %) were dissolved in dry *p*-xylene (6 mL) and stirred at 90−100 °C for 5 h. The solvent was removed in vacuo, and the residue was purified by flash chromatography on silica gel (PE/CH$_2$Cl$_2$ gradient 1:3). The product was precipitated from a CH$_2$Cl$_2$ solution with MeOH to give 120 mg (65%) of a yellow powder. Mp: 155 °C. The product was too air-sensitive in solution for NMR measurements under normal conditions. Anal. calcd for C$_{34}$H$_{32}$N$_2$O$_4$ (532.64): C 76.67, H 6.06, N 5.26. Found: C 76.5, H 6.0, N 5.2.

Cyclic Voltammetry. Cyclic voltammetry measurements were done in dry and oxygen-free solvents (CH$_2$Cl$_2$ and DMSO) with 0.1 M tetrabutylammonium hexafluorophosphate (TBAH) as the supporting electrolyte and with ∼0.001 M substrate under a nitrogen inert gas atmosphere. A conventional three electrode setup was used with a platinum disk working electrode and a Ag/AgCl pseudo reference electrode. The redox potentials were referenced against internal ferrocene/ferrocenium (Fc/Fc$^+$). The long-term reversibility of the processes was checked by performing multi-cycle thin-layer measurements at 10 mV s^{-1}. Digital simulation of the CVs for **1−3** was done with a program by C. Nervi.[57]

Spectroelectrochemistry. The solutions of the cyclic voltammetry experiments were transferred by a syringe into a spectroelectrochemical optical transparent thin-layer cell (optical path length of 100 μm with a gold minigrid working electrode) described in ref 28. UV/Vis/NIR spectra were recorded with a Perkin-Elmer Lamda 9 spectrometer while applying a constant potential to the solution in the thin-layer arrangement referenced against an Ag/AgCl electrode. The potential was increased in 30 mV steps, and spectra were recorded until the two oxidative processes in CH$_2$Cl$_2$ were fully covered. Back reduction was also performed in order to prove reversibility of the whole process in all cases.

Semiempirical Calculations. Optimizations of the radical cations of **1−6** were done at the AM1-UHF level and of the neutral compounds at AM1-RHF level using the MOPAC97 program[58] until a gradient norm of 0.05 was achieved. No symmetry restrictions were applied.

(54) Lambert, C.; Nöll, G.; Schmälzlin, E.; Meerholz, K.; Bräuchle, C. *Chem. Eur. J.* **1998**, *4*, 2129.

(55) For an alternative synthesis via Ullmann coupling, see Thelakkat, M.; Fink, R.; Haubner, F.; Schmidt, H. W. *Macromol. Symp.* **1997**, *125*, 157.

(56) Blatter, K.; Schlüter, A.-D. *Synthesis* **1989**, *5*, 356.

(57) Nervi, C. Electrochemical Simulations Package V 2.4, 1998.

(58) Mopac97, Fujitsu Inc., Japan, 1997.